

Sequential generation of self-starting diverse operations in all-fiber laser based on thulium-doped fiber saturable absorber

Pei Zhang(张沛), Kaharudin Dimyati, Bilal Nizamani, Mustafa M. Najm, and S. W. Harun

Citation: Chin. Phys. B, 2022, 31 (**6**): 064204. DOI: 10.1088/1674-1056/ac3ba9
Journal homepage: http://cpb.iphy.ac.cn; http://iopscience.iop.org/cpb

What follows is a list of articles you may be interested in

Generation of domain-wall solitons in an anomalous dispersion fiber ring laser

Wen-Yan Zhang(张文艳), Kun Yang(杨坤), Li-Jie Geng(耿利杰), Nan-Nan Liu(刘楠楠), Yun-Qi Hao(郝蕴琦), Tian-Hao Xian(贤天浩), and Li Zhan(詹黎)
Chin. Phys. B, 2021, 30 (**11**): 114212. DOI: 10.1088/1674-1056/ac0e22

All-fiber laser seeded femtosecond Yb:KGW solid state regenerative amplifier

Renchong Lv(吕仁冲), Hao Teng(滕浩), Jiajun Song(宋贾俊), Renzhu Kang(康仁铸), Jiangfeng Zhu(朱江峰), and Zhiyi Wei(魏志义)
Chin. Phys. B, 2021, 30 (**9**): 094206. DOI: 10.1088/1674-1056/ac11d3

Analysis of dark soliton generation in the microcavity with mode-interaction

Xin Xu(徐昕), Xueying Jin(金雪莹), Jie Cheng(程杰), Haoran Gao(高浩然), Yang Lu(陆洋), and Liandong Yu(于连栋)
Chin. Phys. B, 2021, 30 (**2**): 024210. DOI: 10.1088/1674-1056/abc3b4

Two-dimensionally controllable DSR generation from dumbbell-shaped mode-locked all-fiber laser

Zhi-Yuan Dou(窦志远), Bin Zhang(张斌), Jun-Hao Cai(蔡君豪), Jing Hou(侯静)
Chin. Phys. B, 2020, 29 (**9**): 094201. DOI: 10.1088/1674-1056/ab9de1

High conversion efficiency, high power density Q-switched fiber laser

Chen Xiao, Xiao Qi-Rong, Jin Guang-Yong, Yan Ping, Gong Ma-Li
Chin. Phys. B, 2014, 23 (**6**): 064218. DOI: 10.1088/1674-1056/23/6/064218

RAPID COMMUNICATION

Sequential generation of self-starting diverse operations in all-fiber laser based on thulium-doped fiber saturable absorber

Pei Zhang(张沛)[1,2,3], Kaharudin Dimyati[3,4], Bilal Nizamani[3], Mustafa M. Najm[3], and S. W. Harun[3,5,†]

[1] *School of Electrical and Information Engineering, Huaihua University, Huaihua* 418008, *China*
[2] *Key Laboratory of Intelligent Control Technology for Wuling-Mountain Ecological Agriculture in Hunan Province, Huaihua University, Huaihua* 418008, *China*
[3] *Department of Electrical Engineering, Faculty of Engineering, University of Malaya, Kuala Lumpur* 50603, *Malaysia*
[4] *Faculty of Advanced Technology and Multidiscipline, Airlangga University, Surabaya* 60115, *Indonesia*
[5] *Institute of Computer Science and Digital Innovation, UCSI University, Kuala Lumpur, Malaysia*

(Received 18 September 2021; revised manuscript received 3 November 2021; accepted manuscript online 20 November 2021)

Self-starting *Q*-switching, *Q*-switched mode-locking and mode-locking operation modes are achieved sequentially in an all-fiber erbium-doped fiber laser with thulium-doped fiber saturable absorber for the first time. The central wavelengths of *Q*-switching, *Q*-switched mode-locking and mode-locking operation modes are 1569.7 nm, 1570.9 nm, and 1572 nm, respectively. The mode-locking operation of the proposed fiber laser generates stable dark soliton with a repetition rate of 0.99 MHz and signal-to-noise ratio of 65 dB. The results validate the capability of generating soliton pulse by doped fiber saturable absorber. Furthermore, the proposed fiber laser is beneficial to the applications of optical communication and signal processing system.

Keywords: all-fiber laser, *Q*-switched mode-locking, dark soliton, fiber saturable absorber

PACS: 42.60.Fc, 42.55.Wd, 42.65.Tg, 42.70.–a **DOI:** 10.1088/1674-1056/ac3ba9

Pulsed fiber lasers have attracted plentiful attention in various applications in the latest decades, due to the abundant advantages including low lasing threshold, simple configuration, high efficiency and low cost. Saturable absorber (SA) is the essential device to realize the pulsed fiber lasers. Various SAs, such as semiconductor saturable absorption mirror,[1] carbon nanotube,[2] graphene,[3] topological insulators,[4,5] black phosphorus,[6] and transition metal dichalcogenides,[7,8] have been studied to achieve mode-locking operation in fiber lasers. These materials are vulnerable to oxidization, which leads to short-term stability.[9] Meanwhile, thermal effects induced by optical power restrict the damage threshold of these SAs.[10]

One of the most effective techniques to address these issues is to employ the doped fiber saturable absorber (DFSA) to realize all-fiber configuration in fiber lasers. In fact, DFSA, a segment of doped fiber inserted in the laser cavity, possesses long-time stability and high damage threshold due to the intrinsic feature of silica glass. Moreover, employing DFSA is the most practical method to manufacture all-fiber pulsed lasers because DFSA is more accessible and convenient to be fabricated massively. To date, DFSA is mostly employed for *Q*-switching pulse generation. For instance, the first all-fiber pulsed fiber laser with DFSA was demonstrated by utilizing 25 cm-long fiber SA doped with chromium, an element of transition metal.[11] Afterwards, DFSAs mainly consist of fibers doped with rare-earth elements, such as erbium,[12] samarium,[13] ytterbium,[14] thulium,[15] and holmium.[16] Recently, bismuth, an element of main group, doped in the fiber was reported as a *Q*-switcher in an all-fiber erbium-doped fiber laser (EDFL).[17]

However, mode-locking operation in pulsed all-fiber lasers based on DFSA have only been reported in two papers. Mode-locking operation in an EDFL by using Tm–Ho co-doped fiber SA was firstly experimentally reported in 2013. *Q*-switching, *Q*-switched mode-locking and continuous mode-locking operations were observed with an external intervention of rotating the polarization controller.[18] Based on the same type of doped fiber, self-starting dual-wavelength *Q*-switching and mode-locking operations were obtained in an EDFL. The pulse duration was 128 ns at high pump power of 166 mW.[19] However, both all-fiber lasers did not obtain any soliton in mode-locking operation. On the basis of these results, we speculate that the relaxation time of DFSA is increased by the intensive interaction between thulium and holmium ions co-doped in the fiber, as thulium and holmium are collectively sharing similar absorption profile in gain spectrum of erbium.[20]

In this paper, a 12 cm-long thulium doped fiber (TDF) SA is spliced in an EDFL cavity for pulse generation in all-fiber configuration. To the best of our knowledge, self-starting *Q*-switching, *Q*-switched mode-locking, and mode-locking operation states are sequentially observed in the proposed fiber

†Corresponding author. E-mail: wadi72@yahoo.com

© 2022 Chinese Physical Society and IOP Publishing Ltd

laser for the first time. In the mode-locking operation, dark soliton with a repetition rate of 0.99 MHz and signal-to-noise ratio of 65 dB is generated with DFSA.

To demonstrate the optical properties of the TDF SA, the characterization of the TDF is shown in Fig. 1. The absorption loss of TDF is measured by a white light source and an optical spectrum analyzer, which is about 3 dB near 1570 nm in Fig. 1(a). The nonlinear saturable absorption of the TDF is measured by a balanced twin detector measurement technique. The modulation depth and the non-saturable absorption are 3.6% and 49%, respectively, as shown in Fig. 1(b). The modulation depth of TDF is relatively low, which may lead to strong pulse shaping and reliable self-starting.

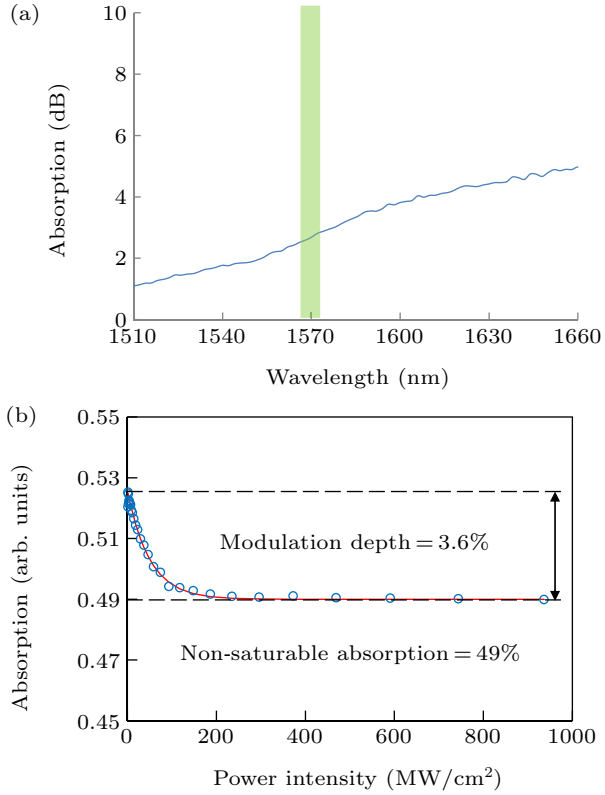


Fig. 1. Characterization of TDF: (a) linear absorption profile, and (b) nonlinear saturable absorption curve.

The experimental setup of the proposed EDFL with an all-fiber ring cavity configuration is illustrated in Fig. 2. A 2.4 m-long erbium-doped fiber (EDF, type I-25) is used as the gain medium and pumped by a 980 nm laser diode pump via a 980/1550 nm wavelength division multiplexer (WDM). The 200 m-long single mode fiber (SMF-28) is incorporated into the cavity to adjust the total cavity dispersion. The TDF is inserted in the cavity as a SA. The unidirectional laser pulse propagation is ensured by a polarization-independent isolator. The 90:10 coupler is inserted into the cavity between the WDM and the isolator. The polarization-dependent losses of couplers, WDM and optical isolator are less than 0.1 dB. Ten percent of generated pulses are drawn out by the coupler and monitored by an optical spectrum analyzer (YOKOGAWA:AQ6370B), an oscilloscope (Yokogawa:AQ6370B), an optical power meter (Thorlabs:PM100D) and a radio frequency spectrum analyzer (Anritsu:MS2683A), respectively. All the components are spliced in the pulsed fiber laser to realize all-fiber configuration. The group velocity dispersion (GVD) plays a crucial part of maintaining stability in mode-locking operation. The GVD of the EDF is -20.3 ps/nm·km and that of the SMF is 16 ps/nm·km, at the wavelength of 1550 nm. In our case, the central wavelength is around 1570 nm, and thus the negligible difference of GVD can be ignored. The total length of the whole cavity is ~ 205 m corresponding to the net cavity dispersion of -4.2 ps^2.

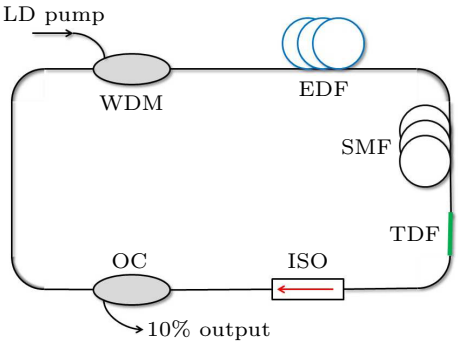


Fig. 2. Schematic of all-fiber pulsed ring laser. LD, laser diode; WDM, wavelength division multiplexer; OC, optical coupler; EDF, erbium-doped fiber; SMF, single mode fiber; TDF, thulium-doped fiber; ISO, isolator.

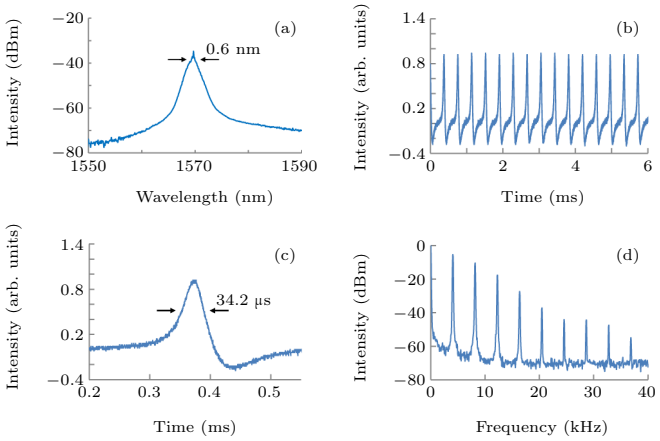


Fig. 3. The Q-switched operation outputs at 23 mW. (a) Optical spectrum of the Q-switched operation, (b) typical Q-switched pulse train, (c) single pulse envelope, (d) the RF spectrum.

The self-started Q-switched pulses occur once the pump power increases to 13 mW, the threshold of continuous-wave lasing. The Q-switched output spectrum at pump power of 23 mW is shown in Fig. 3. In Fig. 3(a), the operating central wavelength is located at 1569.7 nm, with 3 dB bandwidth of 0.6 nm. Figure 3(b) shows the Q-switched pulse train which consists of bright and dark pulses. The repetition rate is 4.05 kHz, corresponding to the time interval of 247 μs. From the profile of the single pulse in Fig. 3(c), we can see that the output pulses have a full width at half-maximum of 34.2 μs with an unsymmetric temporal profile.[21] The corresponding radio frequency (RF) spectrum is measured with a resolution

bandwidth of 10 Hz, as shown in Fig. 3(d). The fundamental frequency is 4.05 kHz, which consistently agrees with the pulse repetition rate. The signal-to-noise ratio (SNR) is over 50 dB, indicating the high stability of the laser output.

Figure 4 depicts the evolution of Q-switching pulse performance as the pump power increases from 13 mW to 23 mW. The evolution of the repetition rate and pulse width with pump power is shown in Fig. 4(a). The pulse width decreases from 55 μs to 34 μs while the repetition rate of the Q-switched pulses increases from 2 kHz to 4 kHz consistently. The average output power and the pulse energy increase from 0.1 mW to 0.46 mW and from 51 nJ to 113 nJ with the rise of pump power, respectively, as noted in Fig. 4(b).

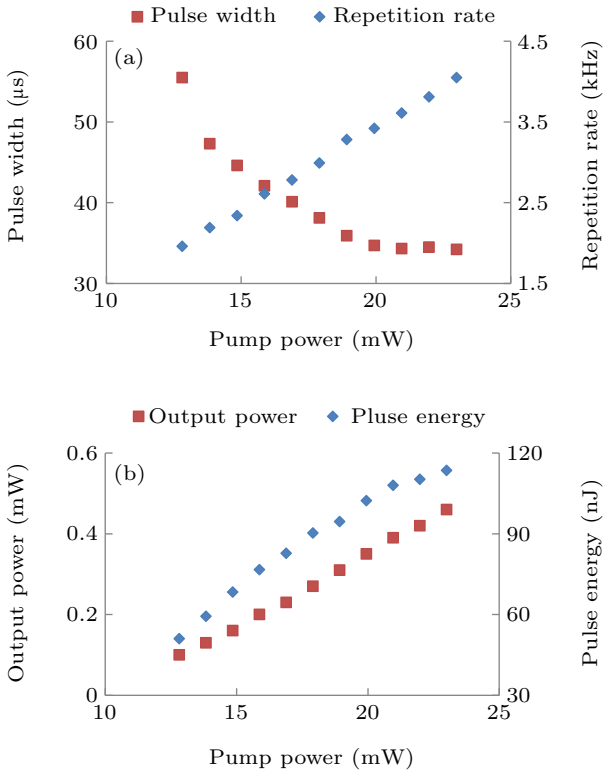


Fig. 4. (a) The pulse duration and repetition rate versus pump power. (a) Average output power and pulse energy versus pump power.

Once the pump power exceeds 23 mW, the Q-switching operation becomes unstable. Further increasing the pump power leads the fiber laser into Q-switched mode-locking (QML) operation, and the Q-switching operation can be recovered again just by decreasing the pump power. The QML pulses are composed of multiple mode-locked pulses which are uniformly sequenced to appear in large Q-switching envelopes. The optical spectrum of QML operation can be seen in Fig. 5(a). The central wavelength is 1570.9 nm with a 3 dB bandwidth of 1 nm. Figure 5(b) shows the QML pulse trains at the pump power of 29 mW. As can be seen, the envelope of the QML pulse train displays a shape similar to the Q-switching pulse in Fig. 3(b). Figure 5(c) shows the typical mode-locking pulses zoomed-in from the image of the QML pulse shown in Fig. 5(b). It can be seen clearly that multiple mode-locking pulses are contained in the Q-switching envelope. The temporal width of the Q-switched envelope is ∼ 63.3 μs, and the time interval between the internal pulses is ∼ 505 ns.

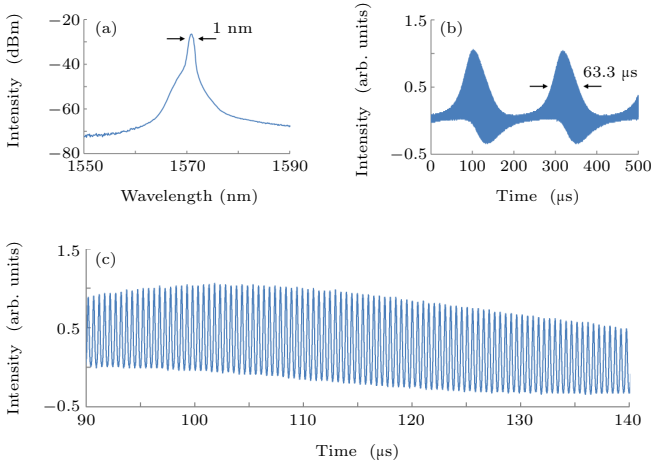


Fig. 5. (a) The QML optical spectrum. (b) Typical QML pulse trains at 29 mW. (c) Magnified view of the single QML pulse.

By continuing to increase the pump power, the proposed fiber laser enters the mode-locking operation. The central wavelength of mode-locking optical spectrum is 1572 nm with 3 dB bandwidth of 0.8 nm, as shown in Fig. 6(a). It is noted that the optical spectrum becomes narrower, and the central wavelength shifts to longer wavelength during the sequential evolution of diverse operations. Due to the increase of pump power, the net increase in gain causes a minor shift in wavelength of about 1 nm towards the longer wavelength.

Due to the cross-phase coupling enhanced by the ascent of pump power, a mode-locking dark pulse train is formed in the cavity. The mode-locking operation can sustain up to the pump power of 41 mW. Figure 6(b) plots the corresponding pulse train which is displayed as intensity dips in an otherwise continuous wave beam of laser emission. Based on numerical simulations, the dark pulse formation is a result of the dark soliton shaping in the fiber laser.[22] As the birefringence is caused by inserting the TDF, the propagating light splits into two orthogonal components. The adjustment of pump power changes the phase difference between the two orthogonal components. The formation of dark soliton derives from the overlap between these two components.[23] Unfortunately, owing to the low repetition rate of the dark pulses, delicate autocorrelation trace cannot be detected in a conventional autocorrelator, and a cross-correlation measurement technique is required. The magnified view of dark pulse is presented in Fig. 6(c). The pulse-to-pulse interval is 1.01 μs, corresponding to the fundamental pulse repetition rate of 0.99 MHz. It is evident that the single pulse envelope only contains dark dip rather than bright pulse. The stability of the dark pulse is further monitored by a RF spectrum analyzer. As shown in Fig. 6(d), the SNR is measured to be around 65 dB at the fundamental frequency

of 0.99 MHz. High SNR and multiple harmonics demonstrate the good stability of mode-locking operation. Compared with bright pulses, researchers have stated that dark pulses are less affected by the power loss and background noise in fiber optical propagation.[24–26] Therefore, dark pulse mode-locking fiber lasers possess great potential for the application in optical communication systems and signal processing.[27,28]. Further increasing the pump power beyond 41 mW leads to unstable pulses which eventually disappear when the laser switches back to continuous wave operation. It is indicated that the SA is oversaturated by the enhancement of pump power.

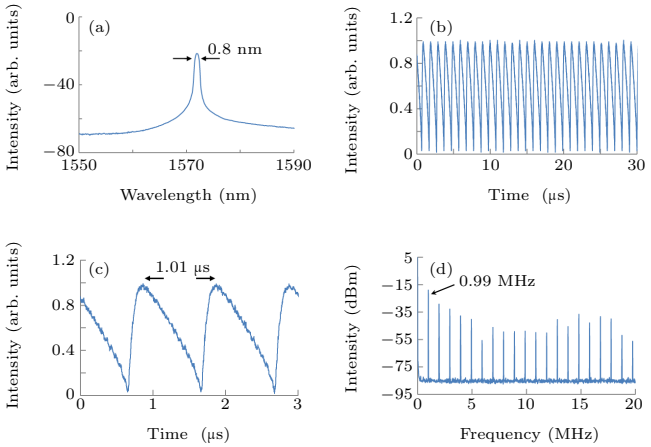


Fig. 6. The mode-locked operation outputs at 41 mW. (a) Optical spectrum of the mode-locked operation, (b) typical mode-locked dark pulse train, (c) magnified view of the dark pulses, (d) the RF spectrum.

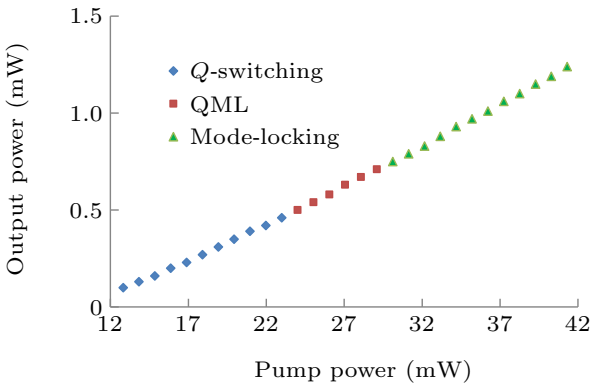


Fig. 7. Output power development against pump power.

The output power development against pump power of proposed all-fiber laser is represented in Fig. 7. The experimental results include three different regimes: Q-switching, QML and mode-locking operations. During the rise period of pump power, the output powers are directly proportional to the pump power and increases linearly without any fluctuation between different regimes. Thus, the slope efficiency of three operation regimes is calculated as same as 4%. Furthermore, the proposed fiber laser has been working steadily for several hours without any interruption in the lab. Different regimes can be operated back and forth while the pump power shuttles slowly between 13 mW and 41 mW.

In summary, we have demonstrated self-starting diverse operations in an EDFL incorporated with DFSA which is prepared by a piece of TDF for the first time. By adjusting the low pump power, Q-switching, QML and mode-locking operations are realized sequentially at 1570 nm region. The output dark soliton with SNR of 65 dB is generated in the mode-locking operation at repetition rate of 0.99 MHz. The experimental results contribute to the development of DFSA in all-fiber mode-locking laser which could find applications in optical communication and signal processing system.

Acknowledgment

This work was supported by the Science and Technology Innovation Program of Hunan Province, China (Grant No. 2021RC5012).

References

[1] Keller U, Weingarten K J, Kartner F X, Kopf D, Braun B, Jung I D, Fluck R, Honninger C, Matuschek N and Der Au J A 1996 *IEEE J. Sel. Top. Quantum Electron.* **2** 435
[2] Lau K Y, Ker P J, Abas A F, Alresheedi M T and Mahdi M A 2019 *Chin. Opt. Lett.* **17** 051401
[3] Fu B, Hua Y, Xiao X, Zhu H, Sun Z and Yang C 2014 *IEEE J. Sel. Top. Quantum Electron.* **20** 411
[4] Miao R, Tong M, Yin K, Ouyang H, Wang Z, Zheng X and Jiang T 2019 *Chin. Opt. Lett.* **17** 071403
[5] Wei Q, Niu K, Han X, Zhang H, Zhang C, Yang C and Man B 2019 *Opt. Mater. Express* **9** 3535
[6] Jin X, Hu G, Zhang M, Hu Y, Albrow-Owen T, Howe R C, Wu T C, Wu Q, Zheng Z and Hasan T 2018 *Opt. Express* **26** 12506
[7] Mak K F and Shan J 2016 *Nat. Photonics* **10** 216
[8] Kadir N, Ismail E I, Latiff A A, Ahmad H, Arof H and Harun S W 2017 *Chin. Phy. Lett.* **34** 014202
[9] Luo Z C, Liu M, Guo Z N, Jiang X F, Luo A P, Zhao C J, Yu X F, Xu W C and Zhang H 2015 *Opt. Express* **23** 20030
[10] Chen C, Yu Y S, Yang R, Wang L, Guo J C, Chen Q D and Sun H B 2011 *J. Lightwave Technol.* **29** 2126
[11] Tordella L, Djellout H, Dussardier B, Saïssy A and Monnom G 2003 *Electron. Lett.* **39** 1307
[12] Tsai T Y, Fang Y C, Lee Z C and Tsao H X 2009 *Opt. Lett.* **34** 2891
[13] Lu Y and Gu X 2013 *Opt. Express* **21** 1997
[14] Lu Y and Gu X 2014 *IEEE Photonics J.* **6** 1
[15] Tiu Z C, Zarei A, Tan S J, Ahmad H and Harun S W 2014 *Chin. Phy. Lett.* **31** 124203
[16] Gene J, Kim S K and Do Lim S 2018 *J. Lightwave Technol.* **36** 2183
[17] Zhang P, Dimyati K, Najm M M, Nizamani B, Paul M C, Das S, Dhar A, Pal M, Yasin M and Harun S W 2021 *Microwave Opt. Technol. Lett.* **63** 2214
[18] Tao M, Wu J, Peng J, Wu Y, Yang P and Ye X 2013 *Laser Phys.* **23** 085102
[19] Latiff A A, Kadir N A, Ismail E I, Shamsuddin H, Ahmad H and Harun S W 2017 *Opt. Commun.* **389** 29
[20] Tao M, Ye X, Wang Z, Yan Y, Feng G, Yang P and Feng G 2014 *Laser Phys.* **24** 085110
[21] Liu Z, Jia W, Wang H, Wang Y, Menke N and Zhang J P 2015 *Chin. Phys. B* **24** 084210
[22] Zhang H, Tang D, Zhao L and Wu X 2009 *Phys. Rev. A* **80** 045803
[23] Kivshar Y S and Turitsyn S K 1993 *Opt. Lett.* **18** 337
[24] Milian C, Skryabin D and Ferrando A 2009 *Opt. Lett.* **34** 2096
[25] Kivshar Y S 1993 *IEEE J. Quantum Electron.* **29** 250
[26] Zhao W and Bourkoff E 1992 *J. Opt. Soc. Am. B: Opt. Phys.* **9** 1134
[27] Zhang H, Tang D, Zhao L and Knize R 2010 *Opt. Express* **18** 4428
[28] Kivshar Y S and Luther-Davies B 1998 *Phys. Rep.* **298** 81